written

$$V_1 = -4\pi \sum_{l,k} \sum_{\substack{l_1 l_2 l_3 \\ l',l'',m}} z_k \frac{\mathbf{d}(^l_k)\cdot\mathbf{r}^0(^l_k)}{|\mathbf{r}^0(^l_k)|^3}(-1)^{l''}(2l+1)\begin{pmatrix} l_1 & l_2 & l' \\ 0 & 0 & 0 \end{pmatrix}^2\begin{pmatrix} l' & l_3 & l'' \\ 0 & 0 & 0 \end{pmatrix}^2 Y_{l''m}^*(\theta_3\psi_3)s^{l_1+l_2+l_3}Y_{l'm}(\theta_2\psi_2)$$

$$+\frac{8\pi^{3/2}}{3^{1/2}}\sum_{\substack{lk \\ l'l''l''',mm''M'''}}\sum_{\substack{l_1 l_2 l_3}} z_k \frac{|\mathbf{d}(^l_k)||\mathbf{r}|}{|\mathbf{r}^0(^l_k)|^3}Y_{1m}^*(\theta_1\psi_1)Y_{l''m''}^*(\theta_3\psi_3)(-1)^{l''}(2l'+1)[(2l''+1)(2l'''+1)]^{1/2}s^{l_1+l_2+l_3}$$

$$\times\begin{pmatrix} l_1 & l_2 & l' \\ 0 & 0 & 0 \end{pmatrix}^2\begin{pmatrix} l' & l_3 & l'' \\ 0 & 0 & 0 \end{pmatrix}^2\begin{pmatrix} 1 & l'' & l''' \\ 0 & 0 & 0 \end{pmatrix}\begin{pmatrix} 1 & l'' & l''' \\ m & m'' & m''' \end{pmatrix}Y_{l'''m'''}^*(\theta_2\psi_2). \quad \text{(A10)}$$

The crystalline potential has been expanded in spherical harmonics. θ_1, θ_2, and θ_3 are the angles between $\mathbf{d}(^l_k)$, $\mathbf{r}$, $\mathbf{r}^0(^l_k)$, and the z direction, respectively. The bracketed terms are $3j$ symbols.

If Eq. (A8) (the ionic shifts) is substituted into Eq. (A10) (crystal field potential), one obtains the frequency dependence as exhibited in the second term on the right side of Eq. (5) and an explicit expression for the $V_{LM}{}^{y,j}$.

Negative Resistance and Impact Ionization Impurities in n-Type Indium Antimonide*

R. J. Phelan, Jr.,† and W. F. Love

University of Colorado, Boulder, Colorado

(Received 2 May 1963)

n-type indium antimonide crystals at liquid-helium temperatures placed in magnetic fields of a few kilogauss have yielded negative resistance characteristics. The negative resistance is attributed to impact ionization of impurities. In addition, delay and rise times for the current have been studied, and an explanation in terms of the rate equation for ionization and recombination is given.

I. INTRODUCTION

THE initial impetus for studying this negative resistance characteristic came from the observation of oscillations of current and voltage generated by single crystals of n-type indium antimonide. These oscillations were previously observed by Haslett and Love[1] while studying the magnetoresistance of n-InSb in pulsed magnetic fields at liquid-helium temperatures. Studies of Sladek[2] and others have indicated that freezeout of the carriers occurs in InSb with the application of a magnetic field at liquid-helium temperatures and with subsequent application of sufficient electric fields impact ionization of the impurities may be obtained. McWhorter and Rediker[3] have demonstrated that impact ionization of impurities in germanium can lead to a negative resistance characteristic. Here we add the observation of negative resistances in n-InSb involving freezeout and impact ionization.

---

[1] J. C. Haslett and W. F. Love, Phys. Chem. Solids 8, 518 (1959).
[2] R. J. Sladek, Phys. Chem. Solids 5, 157 (1958).
[3] A. L. McWhorter and R. H. Rediker, *Proceedings of the International Conference on Semiconductor Physics, 1960* (Czechoslovakian Academy of Sciences, Prague, 1961, Academic Press Inc., New York, 1961), p. 134.

II. SAMPLES

The n-InSb that was used for this study was from three single crystals. The original sample which demonstrated the negative resistance contained few excess donors. A second sample contained 4.6×10^{14} cm^{-3} excess donors and a Hall mobility of 9.1×10^5 cm^2 V^{-1} sec^{-1} at 77°K. The third source was from Cominco and contained relatively few excess donors, 9.5×10^{13} cm^{-3}, and a Hall mobility of 2.7×10^5 cm^2 V^{-1} sec^{-1} at 77°K.

The original sample, shaped into a rectangular bar using a diamond saw, had potential and current leads soldered with indium solder. For the rest of the studies tellurium-doped gold wires were bonded to crystals cut with air-abrasive techniques and the contacts reliably showed linear current-voltage characteristics at liquid-nitrogen temperatures. Contacts were placed at various positions along the bars to check for inhomogeneities. All samples were etched in an attempt to eliminate surface effects.

III. EXPERIMENTAL RESULTS

A. Current-Voltage Characteristics

A typical set of current-voltage curves is given in Fig. 1. This is a Polaroid photograph of two traces of a Tektronix dual beam oscilloscope. Voltages are plotted

vertically and current horizontally. The upper trace gives the Hall voltage versus current, and the lower trace shows the voltage across the potential probes versus the same current. The horizontal scale corresponds to a current density of 0.32 A cm^{-2} per division. The vertical scales for the Hall voltage and potential probe voltage correspond respectively to electric-field intensities of 1.9 and 0.28 V/cm per division. The magnetic field was perpendicular to the sample current and set at an intensity of 4.8 kG. The temperature was 1.1°K. These traces show the symmetric character of

Fig. 3. Relative values of current (horizontally) versus voltage (vertically) for three temperatures, the upper trace corresponds to about 1°K and the lower to about 4°K.
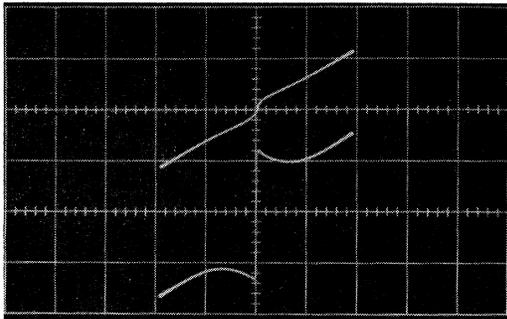
Fig. 1. Hall voltage versus current (upper trace) and sample voltage versus current (lower trace). The vertical scales are, respectively, 1.9 and 0.28 V/cm per division for the upper and lower traces. The horizontal scales both correspond to current densities of 0.32 A/cm^2 per division.

the current-voltage characteristics about the origin of zero current and voltage.

The sample containing 4.6×10^{14} cm^{-3} excess donors did not show a negative resistance for magnetic fields less than 10 kG, while those from Cominco with fewer excess carriers but a lower mobility yielded negative resistance characteristics with a field of 4 kG.

The variation of the current-voltage curves with the change in magnetic field intensity is demonstrated in Fig. 2. For this sequence of oscilloscope traces only a portion of a sine wave was used to display the current-

voltage curves. The current versus time for one of the lower current-voltage curves is given by the upper trace. The magnetic field was perpendicular to the current and had the values of 13.0, 8.5, 4.3, and 0 kG, respectively, from the top to the bottom I-V trace. The temperature for these curves was about 4°K.

The variation of the current-voltage curves with temperature is indicated in Fig. 3. Three curves were

Fig. 4. Breakdown electric field versus breakdown current density.

superimposed from three oscilloscope traces. The maximum temperature was about 4°K and the minimum about 1°K.

The dependence of the current-voltage curves on longitudinal magnetic fields is quite similar to the transverse case except that the onset of negative resistance occurs at lower voltages and is more pronounced since the bulk magnetoresistance is much less.

If one plots the voltages for the onset of negative resistance (the breakdown field) versus the breakdown current density for a transverse magnetic field, one obtains Fig. 4. Taking these same points and plotting the breakdown field versus magnetic field, one obtains Fig. 5.
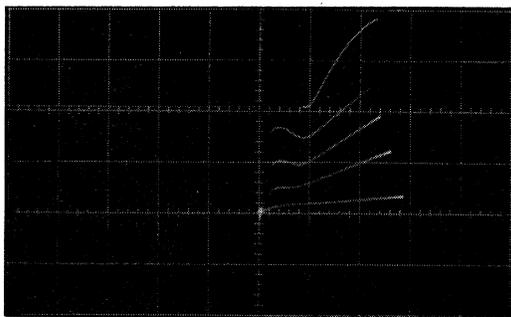
Fig. 2. Relative values of current versus time (upper trace) and current-voltage curves for different values of magnetic field (lower traces). For the upper trace the current is plotted vertically and the time horizontally. For the lower four traces current is horizontal and voltage vertical. The current voltage curves correspond to 13.0, 8.5, 4.3, and 0 kG, respectively, from top to bottom.
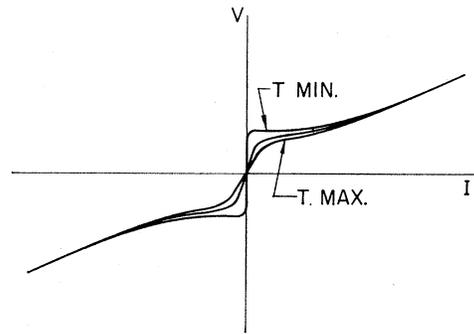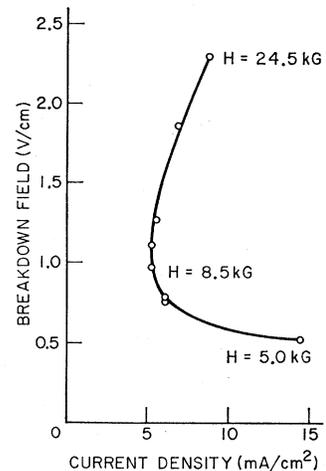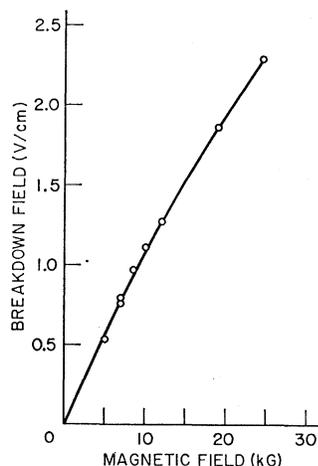
FIG. 5. Breakdown electric field versus magnetic field.

B. Current Versus Time

Upon applying a square pulse of voltage to a crystal, the current showed first a delay and then a rise. In Fig. 6 the upper trace shows the voltage for one pulse corresponding to 0.63 V cm^{-1} of electric-field intensity. The horizontal sweep for this upper beam trace was set at one microsecond per division. The lower set of traces correspond to the current with a vertical scale of 0.29 A cm^{-2} per division and a horizontal scale of 0.2 μsec per division. The temperature was 1.3°K. The magnetic field was parallel to the current and set at the values 0, 3.5, 7.0, 12.0 and 18.5 kG, respectively, from the top to the bottom. A similar sequence of current-versus-time curves was obtained by keeping the magnetic field constant and lowering the applied voltage.

IV. DISCUSSION OF THE RESULTS

A. Current-Voltage Characteristics

Assuming impact ionization of impurities, most of the features of the negative resistance characteristics can be explained. Before a magnetic field is applied no freezeout is observed due to the mergence of the impurity levels with the conduction band. With the application of the magnetic field the impurity levels are separated from the conduction band.[4] With the separation comparable to kT, the electrons become bound to impurity states thus increasing the InSb resistivity. Upon the application of an electric field of sufficient intensity the electrons remaining in the conduction band may acquire enough energy to impact ionize the impurities. With the impact ionization a lowering of the resistivity occurs. If the resistance drops rapidly enough with increasing current, a negative resistance characteristic is observed.

A number of theories have been proposed to explain

[4] Y. Yafet, R. W. Keyes, and E. N. Adams, Phys. Chem. Solids 1, 137 (1956).

the conditions for negative resistance in semiconductors. In the present case it appears that the compensation of donors and acceptors is necessary as was shown to be the case for germanium.[3] The negative resistance was observed in samples with few excess carriers and a reasonable mobility but not observed in samples with a higher concentration of excess carriers and higher mobility. The samples with higher mobility probably had less compensation.

The variation of the Hall voltage with current is consistent with the impact ionization of impurities. As the current is increased the number of carriers increases until all the available impurity states have been ionized. The total number of carriers obtained in this manner is quite close to that obtained by thermally ionizing the impurities by raising the temperature to 77°K. Calculating the carrier density at liquid-helium temperatures from the Hall voltage for currents greater than those of the nonlinear region gave 8.4×10^{13} cm^{-3}. For the same sample in liquid nitrogen 9.5×10^{13} cm^{-3} was obtained. Assuming the 9.5×10^{13} cm^{-3} corresponded to nondegenerate statistics a change to degenerate statistics would affect a change from 9.5×10^{13} to 8.1×10^{13}. It is not obvious with these hot electrons just what statistics should apply, but somewhere between degenerate and nondegenerate seems quite reasonable.

Calculations with assumed thermal conductivities at liquid-helium temperatures indicate that there is negligible heating at the onset of the negative resistance. It is also apparent from Fig. 4 that it is not a given power input that leads to a negative resistance. A breakdown that would correspond to a particular power input would yield a hyperbola for Fig. 4, but the range here is from about 5 to 20 mW/cm^3.

An increase in the breakdown voltage with magnetic field follows from the assumption of impact ionization. In addition to increasing the ionization energy the magnetic field decreases the mobility. Both effects lead to a higher breakdown voltage. To determine quantita-
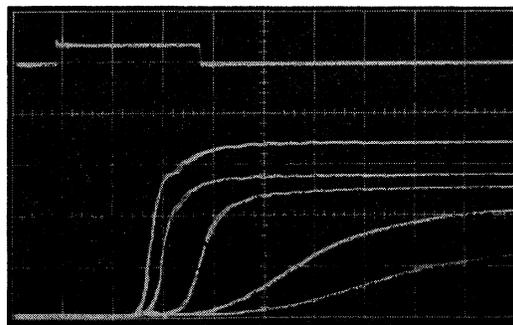

FIG. 6. Pulsed voltage and current versus time. The upper trace shows the voltage vertically corresponding to 0.63 V/cm and a sweep speed of one microsecond per division. The lower five traces show the current vertically at 0.29 A/cm^2 per division with a horizontal scale of 0.2 μsec per division. The current traces correspond to a longitudinal magnetic field of 0, 3.5, 7.0, 12.0, and 18.5 kG, respectively, from top to bottom.

tively the relative influence of the ionization energy and the mobility they would have to be measured separately for these particular crystals.

B. Current Versus Time

The time delays in the rise of the current as shown in Fig. 6 can be explained in terms of the rate equation for impact ionization.

Following the notation of Koenig[5] the rate of change of the number of conduction band carriers is given by

$$\frac{dn}{dt} = A_T(T)(N_D - N_A - n) + nA_I(E)(N_D - N_A - n)$$
$$- nB_T(T,E)(N_A + n) - n^2 B_I(T,E)(N_A + n), \quad (1)$$

where N_D and N_A are, respectively, the densities of donors and acceptors. $A_T(T)$ and $B_T(T,E)$ are, respectively, the thermal coefficients for generation and recombination. $A_I(E)$ and $B_I(T,E)$ are the impact coefficients. The dependence of these coefficients on temperature and electric field is indicated.

In a simplified form, Eq. (1) may be written as

$$dn/dt = a + bn + cn^2 + dn^3, \quad (2)$$

where

$$a = A_T(T)(N_D - N_A),$$
$$b = -A_T(T) + A_I(E)(N_D - N_A) - B_T(T,E)N_A,$$
$$c = -A_I(E) - B_T(T,E) - B_I(T,E)N_A,$$
$$d = -B_I(T,E). \quad (3)$$

If the last term of Eq. (2) is neglected or n is small enough, as was pointed out by Miller,[6] the solution of Eq. (2) may be manipulated into the following form:

$$n = A[1 + B \tanh(t - t_0)/\tau], \quad (4)$$

where

$$A = -b/2c,$$
$$B = (1 - 4ac/b^2)^{1/2},$$
$$\tau = 2/bB,$$

$$t_0 = -(\tau/2) \ln\left[\frac{(b/2c)(B-1) - n_0}{(b/2c)(B+1) + n_0}\right], \quad (5)$$

and n_0 is the value of n at $t = 0$. For low enough temperatures, the coefficient $A_T(T)$ should become quite small. Under this condition one may assume $a/b \ll 1$. With this assumption

$$n = (n_\infty/2)\{1 + \tanh[(t - t_0)/\tau]\}, \quad (6)$$

where

$$\tau = 2/b = 2/A_I(E),$$
$$t_0 = (\tau/2) \ln[(n_\infty - n_0)/n_0], \quad (7)$$

[5] S. H. Koenig, *Solid State Physics in Electronics and Telecommunications* (*Proceedings of the International Conference held in Brussels, June 1958*), edited by M. Desirant and J. L. Michiels (Academic Press Inc., New York, 1960), Vol. 1.

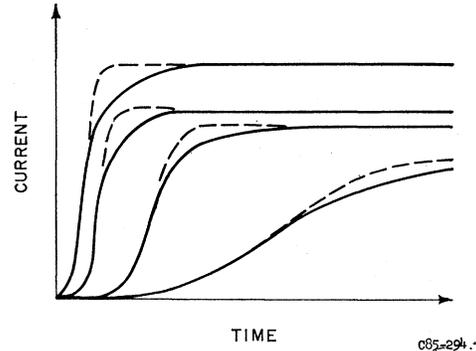[6] S. C. Miller, University of Colorado (private communication).

FIG. 7. Experimental (solid) and theoretical (dashed) curves of current versus time.

and n_∞ corresponds to the steady-state case as $t \to \infty$. Recalling the plot of one plus the hyperbolic tangent of t/τ and shifting the origin by t_0/τ, curves similar to those of Fig. 6 are obtained. The difference between the traces of Fig. 6 (noting that current is plotted and not n versus t) correspond to the change in $A_I(E)$, which is larger for a larger value of the applied voltage minus the breakdown voltage, and changes in n_0. By lowering this overvoltage and lowering the temperature, long delays and sharp rise times can be obtained. Hyperbolic tangents have been fitted to four traces of Fig. 6 and are shown in Fig. 7. Deviations of the current traces from the hyperbolic tangent can be attributed to the loading of the pulse source.

The delays in the current may be more readily observed in compensated material. Assuming that the energy levels are not influenced, greater compensation for a given number of excess donors will yield more complete freezeout at a given temperature. For t_0/τ's of 2, 3, and 4, n_0/n_∞ must be 1.8×10^{-2}, 2.5×10^{-3}, and 3.3×10^{-4}, respectively. The center trace of Fig. 6 corresponds to a t_0/τ of about 3.

V. CONCLUSIONS

The negative resistance in n-InSb has been used to generate 200-kc/sec oscillations and has been shown to have switching capabilities of less than a microsecond. In addition to switching with a voltage pulse across the current leads switching can be accomplished by varying the applied magnetic field.

Possibly through a more thorough study of this impact ionization of impurities in InSb and a correlation of the results with the same phenomena in germanium, a more thorough understanding of the conditions for the negative resistance could be obtained. The degree of compensation appears to be important for both cases.
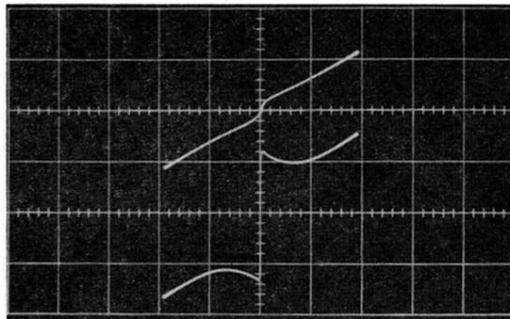
Fig. 1. Hall voltage versus current (upper trace) and sample voltage versus current (lower trace). The vertical scales are, respectively, 1.9 and 0.28 V/cm per division for the upper and lower traces. The horizontal scales both correspond to current densities of 0.32 A/cm² per division.
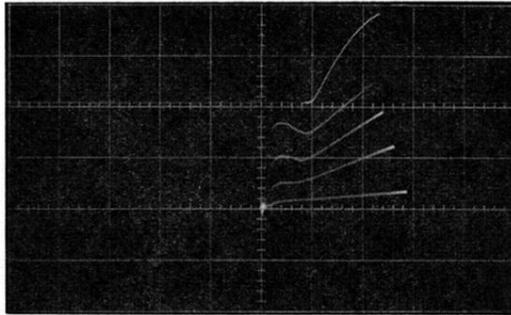
Fig. 2. Relative values of current versus time (upper trace) and current-voltage curves for different values of magnetic field (lower traces). For the upper trace the current is plotted vertically and the time horizontally. For the lower four traces current is horizontal and voltage vertical. The current voltage curves correspond to 13.0, 8.5, 4.3, and 0 kG, respectively, from top to bottom.
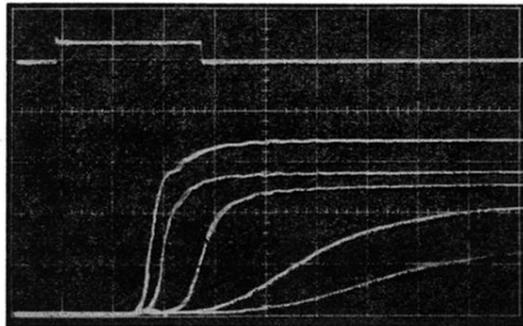
FIG. 6. Pulsed voltage and current versus time. The upper trace shows the voltage vertically corresponding to 0.63 V/cm and a sweep speed of one microsecond per division. The lower five traces show the current vertically at 0.29 A/cm² per division with a horizontal scale of 0.2 μsec per division. The current traces correspond to a longitudinal magnetic field of 0, 3.5, 7.0, 12.0, and 18.5 kG, respectively, from top to bottom.